Development and Application of a New Spray Impingement Model Considering Film Formation in a Diesel Engine

Seong Hyuk Lee
Researcher, Research Institute of Production Engineering, Chung-Ang University, Seoul 156-756, Korea
Gwon Hyun Ko
Ph. D. Candidate, Department of Mechanical Engineering, Chung-Ang University, Seoul 156-756, Korea
Hong Sun Ryou*
Department of Mechanical Engineering, Chung-Ang University, Seoul 156-756, Korea
Ki Bae Hong
Department of Thermal Engineering, Chung Ju University, Chungbuk 380-702, Korea

The present article presents an extension to the computational model for spray/ wall interaction and liquid film processes that has been dealt with in the earlier studies (Lee and Ryou, 2000a). The extensions incorporate film spread due to impingement forces and dynamic motion induced by film inertia to predict the dynamic characteristics of wall films effectively. The film model includes the impingement pressure of droplets, tangential momentum transfer due to the impinging droplets on the film surface and the gas shear force at the film surface. Validation of the spray/wall interaction model and the film model was carried out for non-evaporative diesel sprays against several sources of experimental data. The computational model for spray/wall interactions was in good agreement with experimental data for both spray radius and height. The film model in the present work was better than the previous static film model, indicating that the dynamic effects of film motion should be considered for wall films. On the overall the present film model was acceptable for prediction of the film radius and thickness.

Key Words : Impingement, Film, Spray, Rebound, Deposition, Splash

Nomenclature

N	: Number of drops in a parcel.
N_{drop}, N_{splash}	: Number of incident and splashed droplet parcels, respectively.
K	: Dimensionless parameter for impingement.
K_f	: Friction factor.
D	: Drop Diameter.
Oh	: Ohnesorge Number ($=\mu_d/\sqrt{\rho_d\sigma_d D_b}$).
Re	: Reynolds Number ($=\rho_d D_b \nu_{bn}/\mu_d$).
r_m	: Mass ratio.
S_M, S_{ud}, S_{vd}	: Depth-averaged source terms of continuity and momentum of films.
$U_{d,n}, U_{g,n}$	: Normal component of droplet velocity.
$\bar{u}$, $\bar{v}$	: Depth-averaged velocity components
We	: Weber number
μ	: Viscosity
θ	: Void fraction
ρ	: Density
σ	: Surface tension
τ_s, τ_w	: Shear stress at interface and wall, respectively.

* Corresponding Author,
E-mail : cfdmec@cau.ac.kr
TEL : +82-2-820-5280 ; **FAX** : +82-2-814-9476
Department of Mechanical Engineering, Chung-Ang University 221, Heuk Suk-dong, Dong Jak-ku, Seoul 156-756 Korea. (Manuscript **Received** March 2 2000; **Revised** April 19, 2001)

Ψ : Time fraction at which the splash occurs

Subscripts

a : After impingement
b : Before impingement
d : Droplet
f : Film
g : Gas phase
n : Normal direction
t : Tangential direction

Superscripts

T : total velocity

1. Introduction

Generally, films built on the wall from spray impingement is an important process in small bore DI diesel engines where sprays unavoidably impinge on the piston wall, and in gasoline engines with port-fuel injection, where fuel is deposited on the surfaces of intake valves, ports or cylinders. In such situations, the behavior of impinging sprays and wall films has a great influence on the mixture formation and combustion processes. For instance, incomplete evaporation and burning of wall films in diesel engines may enhance soot formation and increase unburnt hydrocarbon emission. In particular, as noted by Gonzales et al. (1991), the film characteristic due to the spray impingement should be understood in order to enhance the cold-starting performance of diesel engines and also to prevent a misfire (Zahdeh et al., 1990). It is therefore important to identify the major parameters which affect wall film spreading and determine the optimum operating conditions. Better understanding of the mechanisms governing spray impingement and film dynamics will help achieving this goal.

Computational modeling offers a promising alternative to obtain the detailed information such as the local velocities and Sauter mean diameter (SMD), that is difficult to measure in the near wall region. That is why computational modeling is considered as an important part of the performance analysis together with the experimental work. Several some investigators have reported the computational models for spray/wall interactions and film movement. Yoshikawa et al. (1993) performed 3-D modeling of spray-valve interaction and observed extensive drop interaction between induction port and intake valve. This interaction is an important contribution to liquid atomization and vaporization. Nagaoka et al. (1994) used a particle film model in 3D calculations of SI engines. However their model could not predict the transient behavior of the wall film effectively because of the assumption that the wall film does not move. Meanwhile, it turned out that splash is an important physical phenomenn in small-bore, direct-injected gasoline and diesel engines, as well as in a variety of other industrial devices in which sprays impinge on solid surfaces. Lee and Ryou (2000b) carried out comparisons of the earlier published models (Watkins and Wang, 1990; Park, 1994; Bai and Gosman, 1995) for spray/wall impingement with several sources of experimental data. They modified the impingement model for effective prediction of the post-impingement characteristics. They showed that some of the earlier published models significantly underestimated the height of wall sprays and indicated that this problem results from the fact that the splash effect is not included in these models based on the hot wall data of Wachters and Westerling (1966). In recent literatures, some efforts to complement this problem have been reported for effective prediction of splash and wall films (Bai and Gosman, 1995; Stanton and Rutland, 1996; Mundo et al., 1998). In particular, the authors have suggested the spray/wall interaction model including the static model of wall films (Lee, 1999; Lee and Ryou, 2000a). The spray impingement model consists of several mathematical formulae, derived from the energy conservation law and experimental results. It includes the three representative regimes, rebound, deposition and splash regome. The wall films model may be called "a static model," since it is basically derived from the earlier research of Nagaoka et al. (1994), and modified to consider the transient behavior. Although the spray/wall interaction model showed good predictions in these studies, the

results showed that the static film model significantly underestimated the film penetration in the radial direction and subsequently failed to predict the dynamic characteristics of wall films. Although there are several previous researches as mentioned in the above, few 3D codes allow liquid film formation and spray/wall interactions, up to now. Most of the computational models may still be considered as a work-in-progress and more comparisons are required for validation. Hence, it is important to develop a reliable numerical model for spray/wall interactions and film formation and to validate against various test cases related to DI diesel engines.

The present article presents an extension to the computational model for spray/ wall interactions and liquid film processes in the earlier studies (Lee et al., 2000a). In order for more efficient description of wall films, the film spreading due to impingement forces and the dynamic motion due to film inertia are considered for prediction of the dynamic characteristics of wall films. The transport equations of mass and momentum of wall films are established under the boundary -layer assumption and solved by a combination of integral and differential methods, a two-dimensional framework. The aim of this study is the investigate spray-film impingement, liquid film formation and post-impingement processes as related to DI diesel engines. Consequently, droplet impingement on cold and wetted wall is examined along with post-impingement processes including splashing phenomena. The cold wall' means one with the temperature below the fuel boiling point. The film spreading characteristics and the fuel film thickness may provide insight into spray wall interactions in cold starting. Assessment of the models presented here was carried out for non-evaporative diesel sprays by comparing their predictions against experimental data.

2. Mathematical Representation of the Film Model

2.1 The static model of wall films

So called "the lens model" proposed by Nagaoka et al. (1994) could not take account of the transient behavior of wall films because it was assumed that the liquid film did not move. In addition, it did not describe the spray-film interaction, resulting in partial contribution of impinging droplets to wall films. As an effort to resolve this problem, Lee (1999) proposed the static model for predicting transient behavior of films by modifying the lens model of Nagaoka et al. (1994). The film mass deposited on the wall can be represented as a summation of two parts.

$$m_{rem}=\sum_i N_i\rho_{d,i}\pi D_{b,i}^3/6 + \sum_i N_i(1-r_m)\,\rho_{d,i}\pi D_{b,i}^3/6 \qquad (1)$$

On the right-hand side of Eq. (1), the first term is the mass of droplets deposited on the wall and the second is the mass of droplets added or subtracted due to the splash. The empirical relationships which have been used by Nagaoka et al. (1994) are used identically in the static model to determine the film radius and thickness remaining on the wall. However, it is difficult to describe the film radius and thickness from the lens model because the model cannot predict successively the varying position of the film as time goes on. In order to complement this problem, we assumed an artificial droplet, which is of the equivalent diameter, which is defined as the droplet diameter of spherical shape corresponding to the film mass at a certain time. The film formation process is described by using the assumption that, during the time step, the incident droplet with the equivalent diameter adheres to the wall and attains a stable circular disk shape, which is affected by interaction between gravity and surface tension effects. In the static model, the film built on the wall is assumed to be circular disk and simplified as shown in Fig. 1. The relationship between radius and thickness of the film is $h_f/2r_f=0.0177\,E_0^{-0.51}$ (Xiong and Yuen, 1991) where h_f represents the thickness from the wall to the top of film having the lens shape as shown in Fig. 1. The Eotvos number, E_0, describes that the droplet resting on a surface depends on the equilibrium between gravity and the effects of its surface tension. From geometrical consideration, the

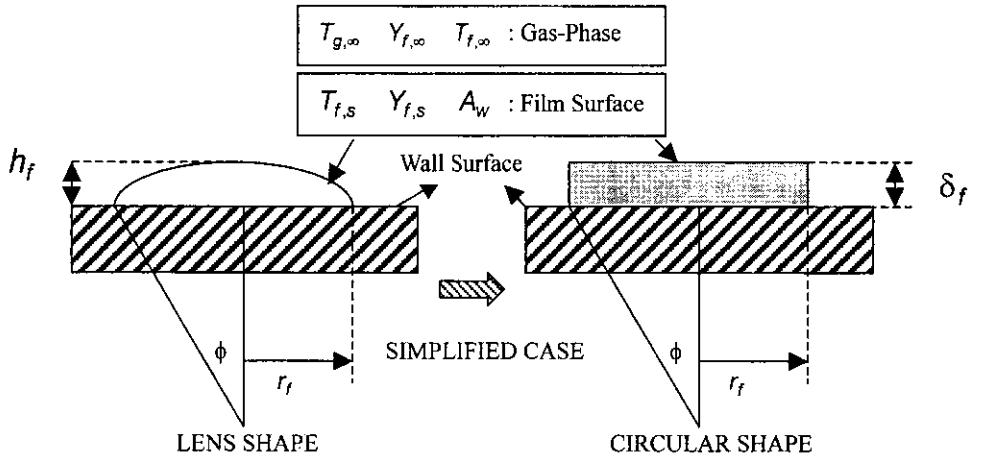

Fig. 1 Schematic diagram of the present film model

radius of film being the lens shape is determined as follows.

$$r_f=\sin\phi^3\sqrt{\frac{3\forall_f}{\pi(2-3\cos\phi+\cos^3\phi)}} \qquad (2)$$

where ϕ is obtained from the geometric relationship. The film thickness, δ_f, is used in the static model on the assumption of circular disk to simplify the film shape and is given by $m_{rem}/\rho_d\pi r_f^2$. A shortcoming of this model is that the model is roughly based on some of unrealistic assumptions. As will be referred below, the static model shows significant underestimation of the radius of wall films. As an effort of solving this problem, the dynamic model for wall films will be discussed in what follows.

2.2 The dynamic model of wall films

A major challenge to the modeling of the wall film behavior is the need to cope with the interface between the liquid and the gas, and to track the moving contact line. Thus far, this interface has been viewed in two ways, i. e., the macroscopic view and the microscopic view according to Bai (1996). In this study, the macroscopic view of the interface is adopted because of its relative mathematical simplicity and the fact that the jump conditions arising from this provides boundary conditions in a straightforward way for problems involving dynamic phase changes. The film model includes the impingement pressure of droplets, tangential momentum transfer due to the impinging droplets on the film surface and the gas shear force at the film surface. The following assumptions are used in the formulation of the film model.

1) The mass flux due to incident impinging droplets is averaged over the wall cell area

2) Lost tangential momentum of impinging droplets is added to the film tangential momentum

3) The liquid film flow is laminar according to Stanton and Rutland (1996) and Bai (1996) and it is assumed to be thin enough so that the incompressible boundary layer approximations can be applied.

The solutions of the film equations are to be sought using a combination of integral and differential methods. This avoids the need for discretisation of a three-dimensional domain, thus also avoiding the need to adjust the grid to follow the moving and deforming film interface. It also enables the reduction of the order of the governing differential equations and thereby facilitates simple numerical solutions. The continuity equation can be rewritten as below after integration with the aid of the jump balance equation.

$$\frac{\partial\delta_f}{\partial t}+\frac{\partial}{\partial x}(\bar{u}\delta_f)+\frac{\partial}{\partial y}(\bar{v}\delta_f)=\frac{S_M}{\rho} \qquad (3)$$

Also, the film momentum equations are as follows.

$$\frac{\partial(\bar{u}\delta_f)}{\partial t}+\frac{\partial}{\partial x}(C_1\bar{u}\bar{u}\delta_f)+\frac{\partial}{\partial y}(C_2\bar{u}\bar{v}\delta_f)$$

$$= -\frac{\delta_f}{\rho}\frac{\partial p}{\partial x} + \frac{1}{\rho}(\tau_{sx} - \tau_{wx}) + \frac{S_{ud}}{\rho} + \delta_f g_x \quad (4)$$

$$\frac{\partial(\overline{v}\delta_f)}{\partial t} + \frac{\partial}{\partial x}(C_2 \overline{u}\,\overline{v}\delta_f) + \frac{\partial}{\partial y}(C_3 \overline{v}\,\overline{v}\delta_f)$$

$$= -\frac{\delta_f}{\rho}\frac{\partial p}{\partial y} + \frac{1}{\rho}(\tau_{sy} - \tau_{wy}) + \frac{S_{vd}}{\rho} + \delta_f g_y \quad (5)$$

The total pressure consists of three parts as follows.

$$p = p_d + p_g + p_\sigma \quad (6)$$

The capillary pressure, p_σ, which arises from surface curvature was neglected in the present study according to a non-dimensional study carried out in Foucart et al. (1998). The impact pressure and the gas pressure are determined from the following expressions (Bai, 1996).

$$p_d = (1-\theta)\rho U_{d,n}^2 ran(1,0) \quad (7)$$

$$p_g = 0.5\theta\rho U_{g,n}^2 \quad (8)$$

where ran(1, 0) represents a random number distributed uniformly between 0 and 1. The liquid film is locally subject to a total pressure at the interface. Under the boundary-layer approximations, the local pressure within the film can be taken constant across the film depth. The constants C_1, C_2 and C_3 represent coefficients arising from the integration and in the present study, the linear profile was assumed for film velocity. In above equations, S_{ud} and S_{vd} represent the tangential momentum contribution to the film. For instance, the source term S_{ud} in the x direction is as follows.

$$S_{ud} = \sum_{i}^{Ndrop} m_i'' V_{di,x} - \sum_{j}^{Nsplash} m_j'' V_{dj,x} \quad (9)$$

where m'' is the mass flux due to the impinging droplets over the film area and $V_{di,x}$ is the x component of droplet velocity. For each regime of impingement, the loss of tangential momentum is determined as follows

$$\frac{\pi\rho_f}{6A_f\Delta t}\sum_{k}^{Ndrop}\left(N_k d_k^3 \frac{2}{7} V_{t,dk}\right) \text{ For Rebound} \quad (10)$$

$$\frac{\pi\rho_f}{6A_f\Delta t}\sum_{k}^{Ndrop}\left(N_k d_k^3 V_{t,dk}\right) \text{ For Deposition} \quad (11)$$

$$\frac{\pi\rho_f}{6A_f\Delta t}\left[\sum_{k}^{Ndrop}\left(N_k d_k^3 V_{t,dk}\right) + \sum_{j}^{Nsplash}\left(N_j d_j^3 V_{t,dj}\right)\right] \text{ For Splash} \quad (12)$$

The film initial conditions are specified at the time at which impingement commences. Here we assumed that there is an immediate formulation of a film patch, which has an area A_f determined by the positions of either adhesion or splashing droplets. The film thickness is assumed to be uniform over this area and it is determined by the total volume of the deposited fuel divided by the area. The initial film layer is assumed to possess no inertia, but has the momentum sources imparted by the droplets, and is subject to the impact pressure as well.

2.3 Spray-wall interaction model

The main features of the new model are in the usage of regime criteria based on consistent experimental results, in the determination of the post-impingement characteristics based on energy conservation law and experimental results, and in the methodology on the transient behavior of film built on the wall. The deposition-splashing boundary is determined in the model from empirical correlation proposed by Mundo et al. (1995) as follows.

$$K = Oh\mathrm{Re}^{1.25} = 57.7 \quad (13)$$

where K is dimensionless parameter for impingement, expressed in terms of Reynolds and Ohnesorge numbers. The main feature of this model is in the determination of the total velocity of droplets after impingement by using the newly derived relationship for the dissipated energy instead of the critical Weber number, deduced from the experimental consideration. We can obtain the relationship for the total velocity of ejected droplets as follows.

$$We_a^T = \frac{C_w We_b^T}{\gamma_m} - \left(\frac{4.5 \cdot C_w We_{bn}\gamma_{\max}^4}{\gamma_m \mathrm{Re}_{bn}} - \frac{12 C_w}{\gamma_m}\right) - 12 \quad (14)$$

where $\gamma_{\max}$ is the dimensionless parameter of the disc when splashing occurs. The tangential velocity of splashed droplets can be derived from the theoretical relationship of Yarin and Weiss (1995) as follows.

$$v_f = 0.452 K_f \cdot \mathrm{Re}_{bn}^{1/8} \cdot v_{bn} / \sqrt{\Psi} \qquad (15)$$

where Ψ represents the time fraction which is defined as the ratio of time when the splash occurs to the residence time of an incident droplet. To consider the effect of viscosity, we introduce the friction factor, K_f, which is randomly chosen in the range between 0.81 and 0.91 (Yarin and Weiss, 1995). See the reference (Lee, 1999; Lee and Ryou, 2000a) for more details.

3. Numerical Method

The gas phase is derived in terms of the Eulerian conservation equations and turbulent transport is modeled by the modified k-ε model of Reynolds (1980). To couple between the gas phase velocity and the pressure field, the implicit and non-iterative PISO algorithm is used in the present study. The gas phase transport equations are discretized by finite volume method. With this process, the Euler implicit method is used for the transient term, and a hybrid upwind/central difference scheme is used to approximate the convection and diffusion terms. The droplet parcel equations are written in Lagrangian form. The ordinary differential Lagrangian equations for the droplets are also discretised in the Euler implicit manner. Additionally, the present study incorporates a breakup model widely used for the breakup of liquid droplets in a gaseous stream proposed by Reitz and Diwakar (1987), where two breakup regimes are identified as the bag and stripping breakup. Also, the collision and coalescence model of O'Rourke (1981) is used in this paper.

Briefly, let us introduce the numerical methodology for calculating the film movement. The film calculation was conducted by means of a predictor-corrector scheme. For example, the predictor-corrector scheme for continuity equation of films includes the Euler method as a predictor. :

$$\delta^* = \delta^n - \frac{\Delta t}{A_f} \sum_i^{NSIDE} (V_f^n \cdot n)\, \delta_i^n l_i + \frac{\Delta t S_M}{\rho} \qquad (16)$$

followed by the trapezoid rule as a corrector :

$$\delta^{n+1} = \delta^n - \frac{\Delta t}{A_f} \sum_i^{NSIDE} (V_f^{**} \cdot n)\, \delta_i^{**} l_i + \frac{\Delta t S_M}{\rho} \qquad (17)$$

where ** means the averaged value between the old and the predictor steps. At the edges of the film, an upwind scheme is used and all film variables are cell centered quantities. The momentum equation is solved using the same predictor-corrector method. In computation, the initial film thickness can be calculated by dividing the volume of impinging droplets by a total amount of film area determined by the positions of either adhesion or splashing droplets. Initially, we assumed that the initial film spot occurs when the film thickness is greater than 2.0 μm (Zhengbai et al., 1990).

4. Results and Discussion

This article deals with totally three cases for assessment of the spray/wall interaction model including the film formation as listed in Table 1. Numerical simulations for non-evaporative impinging sprays were performed using the new spray/wall interaction model considering liquid film formation. Figure 2 shows the computational domain for all cases with a $50 \times 50 \times 40$ (x, y and z respectively) grid. This mesh arrangement was found to reduce the grid-size sensitivity of the results (Lee, 1999). As seen in Table 1, Cases 1 and 2 show the experimental conditions used by Katsura et al. (1989) to simulate the overall structure of the non-evaporative impinging sprays. Final test is Case 3 from which results were compared with experimental data of Saito et al. (1993) to validate the present film model. For all test cases, a time step of 10 μs is adopted and in Case 1, a total of 4000 droplet parcels are introduced through injection duration time. For Cases 1 and 2, we used the model of Reitz and Diwakar(1987) to describe the breakup process of liquid jets at the nozzle exit. Reitz(1987) applied the wave stability atomization theory to diesel spray modeling, by injecting parcels of liquid in the form of "blobs" that had a characteristic size equal to the nozzle hole diameter,

Table 1 Specifications of the test cases

Test Case	1	2	3
Impingement Distance [mm]	24	34	25
Gas Pressure [MPa]	1.5	1.5	2.1
Gas Temperature [K]	293	293	293
Wall Temperature [K]	293	293	293
Nozzle Diameter [mm]	0.3	0.3	0.25
Injection Pressure [MPa]	14	14	30
Injection Duration Tiem [ms]	1.2	1.2	2.85
Reference	Katsura et al., 1989	Katsura et al., 1989	Saito et al., 1993

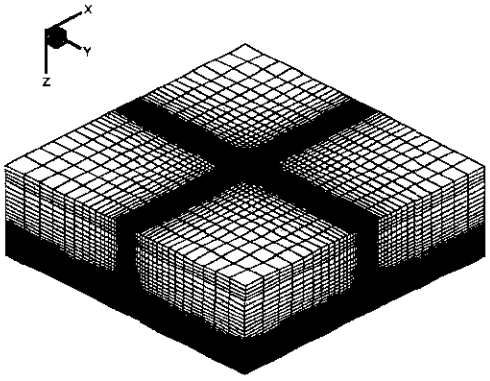

Fig. 2 Grid generation of the present study

instead of assuming an intact liquid at the nozzle exit. The basis of this model is the concept introduced by Reitz and Diwakar(1987) that atomization of the injected liquid and the subsequent breakup of droplets are indistinguishable processes within dense spray. The schedules of injection velocity for Cases 1 and 2 were determined by the curve-fitted relationship from the experimental data produced by Katsura et al. (1989). However, the velocity schedules for Case 3 were assumed by constant velocity based on the experimental condition because it could not be found from the related reference (Saito et al., 1993).

In this paper, the main parameters for comparisons are the radius and the height of wall sprays after impingement. For Cases 1 and 2, Katsura et al. (1989) conducted experiments in which a single spray was normally impinged on a flat plat at high trap pressure and room temperature. As seen in Fig. 3 showing the predicted spray patterns for Cases 1 and 2 at 0.7 ms, the decrease of spray radius can be found as the impingement distance increases, indicating that a longer time is needed for the spray to reach the wall prior to impingement. Figure 4 shows that the calculated results are in good agreements for spray height and radius, with maximum error 7.6 % for Case 1 and 1.6 % for Case 2. This result suggests that the current model can effectively predict the behavior of splashing droplets. It can be observed that at the early stage after start of impingement, the spray radius results are in good agreement with the experimental data. However, the present model under-predicts the spray radius at the later stage of injection. Maximum error is about 12.1 % and 11.6 % for Case 1 and Case 2, respectively, at the end of the total calculation time. This discrepancy is larger toward the end of the injection duration, and caused by the modeling of the droplet size distribution after impingement. The distribution being involved in the new model is based on the experimental data of Naber and Farrell(1993). For the very high Weber number, this distribution may produce smaller droplets than those in the actual phenomena. In this case, smaller droplets ejected due to the impingement cannot penetrate in the radial direction effectively because of insufficient inertia of ejected droplets. Therefore, it is thought that more accurate experimental data for the size distribution of ejected droplets are required in order to produce better prediction. For Case 3 as seen in Fig. 5, very good agreement is observed for the wall-spray radius and height, indicating that the transient

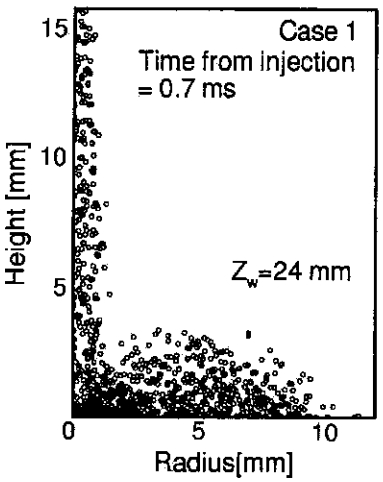

(a) Case 1

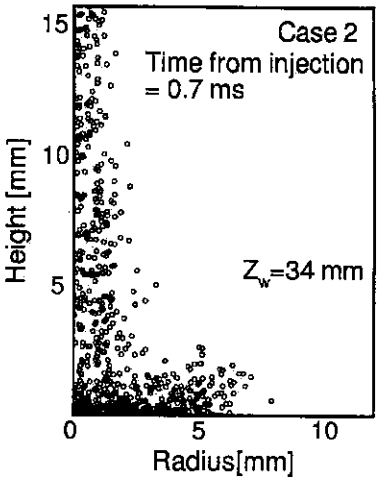

(a) Case 2

Fig. 3 The predicted spray patterns for Cases 1 and 2

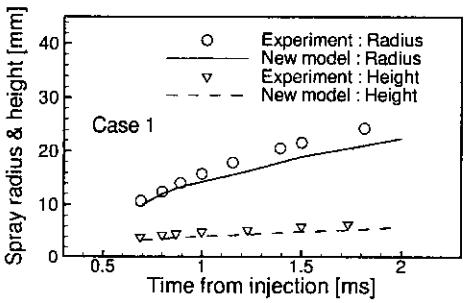

(a) Impingement Distance=24 mm

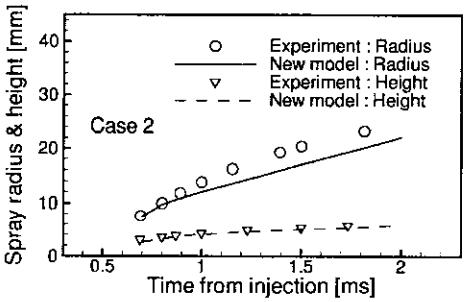

(b) Impingement Distance=34 mm

Fig. 4 Comparisons of the predicted radius and height of wall sprays with experimental data (Katsura et al., 1989) for Cases 1 and 2

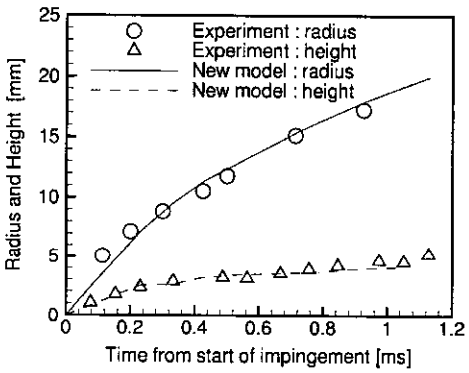

Fig. 5 Comparisons of the predicted radius and height of wall sprays with experimental data (Saito et al., 1993) for Case 3

behavior of wall sprays can be effectively predicted by the present model.

Figure 6 shows the contours of liquid film distribution for different times. As time goes on, the liquid films are propagating along with the radial direction but the incomplete symmetric contours can be seen initially. This is because the tangential and the pressure sources in the film momentum equations are mainly affected by the post-impingement characteristics, which are of random features. Nevertheless, as time goes on, the symmetric shapes can be observed roughly. The film thickness profiles are show in Fig. 7 for various times after the start of impingement. The area around the stagnation point of the spray is immediately flooded. The large film thickness in this regime is due to the impingement of the dense spray region that has not experienced significant breakup. This occurs within a 1.5 mm radial distance. The concaved film profile extending

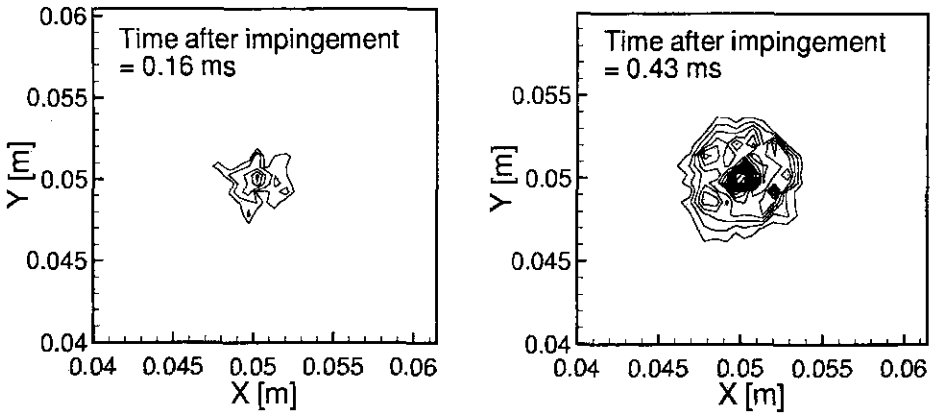

Fig. 6 Contours of wall films at 0.16 and 0.43 ms after impingement for Case 3

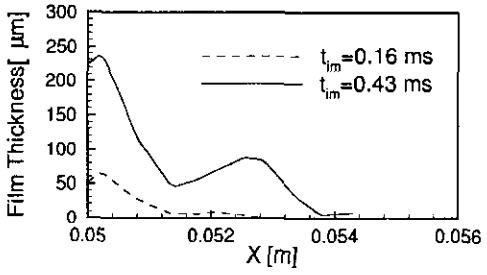

Fig. 7 Predicted film thickness distributions at different times for Case 3

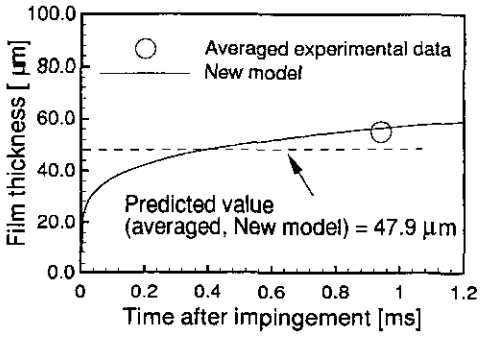

(a) Film Thickness

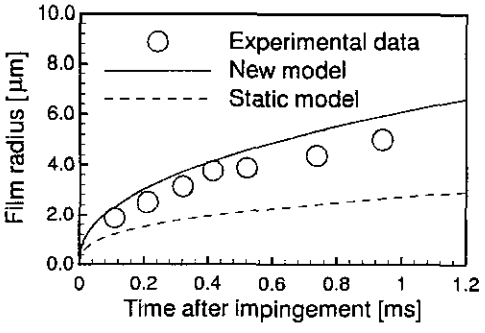

(b) Film Radius

Fig. 8 Comparison of the predicted film height and radius with experimental data (Saito et al., 1993) for Case 3

from the stagnation region at a radial distance of 1.5 mm to a transient peak value is present. This is the result of two primary phenomena. First, a liquid wall-jet is formed at the onset of impingement in this region, which widens in the radial direction causing the liquid wall-jet to decelerate. Second, the film experiences the majority of the spray-film interaction in this region, which results in splashing of secondary droplets, thus reducing the amount of mass in the film. Consequently, it is instructive to investigate droplet velocities in this region, in order to assess the ability of the spray-film model to predict the splashing events.

Comparisons of the mean film radius and the mean film thickness are presented in Fig. 8. The mean film thickness is defined as the total amount of liquid volume by surface area covered by the film. This area is determined by the positions of either adhesion or splashing droplets. Also, the averaged value in Fig. 8 is obtained by averaging the mean film thickness during a total time of calculation. As shown in Fig. 8(a), the new model slightly under-predicted the averaged film thickness, while the static model overestimated it (Lee, 1999). This difference may be due to the calculated radial penetration is slightly overestimated as seen in Fig. 8(b), in spite of the fact

that the deposited film mass, which are calculated from the spray/wall interaction model, is identical for both two models. For film penetration in the radial direction, we can see that the present model is in better agreement with experimental data than the static model. This is because the latter model is based on the static film concept while the former is dealing with the behavior of moving films by solving their governing equations. Although the discrepancy between overestimated film radius and the experimental data increases as time goes on, the present film model is acceptable for prediction of the film radius and thickness, relative to the static model. It might be thought that the dynamic film model presented here may be useful for predictions of global trends of wall films, in spite of some problems in the view of accuracy. To overcome this problem and obtain more accurate predictions, more elaborated study is required. Our future work is to validate the present film model by performing numerical simulations for much more cases in open literature.

5. Conclusions

An extended computational model for spray/wall interaction and film flows has been developed in this paper. A new submodel was tested against several experimental data and the previous impingement models. The following conclusions were drawn. First, the new spray/wall interaction model produced good prediction of the spray height with slight overestimations in the spray radius. Therefore the new spray/wall interaction model is useful for predictions of transient behavior of impinging sprays. Second, for prediction of film radius, the dynamic model presented here is in better agreement with experimental data than the static model. However, the film radius is slightly overestimated, as time goes on. On the overall the present film model is more reliable for prediction of global trends of wall films, than the static model. It is important to note that the film model in this article may still be considered as a work-in-progress, and is expected to undergo further revisions in the future.

Acknowledgement

This work was supported by Korea Research Foundation Grant (KRF-99-041-E00075).

References

Bai, C, 1996, Modeling of Spray Impingement Processes, Ph. D Thesis, Department of Mechanical Engineering, Imperial College of Science, Technology & Medicine, University of London.

Bai, C and Gosman, A. D., 1995, "Development of Methodology for Spray Impingement Simulation," SAE950283.

Foucart, H., Habchi, C., LeCoz, J. F., and Baritaud, T., 1998, "Development of a Three Dimensional Model of Wall Fuel Liquid Film for Internal Combustion Engines," SAE980133.

Gonzalez, M. A., Borman, G. L. and Reitz, R. D., 1991, "A Study of Diesel Cold Starting using Both Cycle Analysis and Multidimensional Calculations," SAE910180.

Katsura, N., Saito, M., Senda, J. and Fujimoto, H., 1989, "Characteristics of a Diesel Spray Impinging on a Flat Wall," SAE890264.

Lee, S. H., 1999, Development of a New Model and Heat Transfer Analysis of Impinging Diesel Sprays on a Wall, Ph D. Thesis, Department of Mechanical Engineering, Chung-Ang Univerisity.

Lee, S. H. and Ryou, H. S, 2000a, "Modeling of Diesel Spray Impingement on a Flat Wall," *KSME International Journal*, Vol. 14, No., 7, pp. 796~806.

Lee, S. H. and Ryou, H. S., 2000b, "Comparison of Spray/Wall Impingement Models with Experimental Data," *Journal of Propulsion and Power*, Vol. 16, No. 6, pp. 939~945.

Mundo, C., Sommerfeld, M. and Tropea, C., 1995, "Droplet-Wall Collisions : Experimental Studies of the Deformation and Breakup Process," *International Journal of Multiphase Flow*, Vol. 21, pp. 151~173.

Mundo, C, Sommerfeld, M. and Tropea, C., 1998, "On the Modeling of Liquid Sprays Impinging on Surfaces," *Atomization and Sprays*, Vol.

8, pp. 625~652.

Naber, J. D. and Reitz, R. D., 1988, "Modeling Engine Spray/Wall Impingement," SAE880107.

Naber, J. D. and Farrell, P., 1993, "Hydrodynamics of Droplet Impingement on a Heated Surface," SAE930919.

Nagaoka, M., Kawazoe, H. and Nomura, N., 1994, "Modeling Fuel Spray Impingement on a Hot Wall for Gasoline Engines," SAE940525.

O'Rourke, P. J., 1981, *Collective Drop Effects on Vaporizing Liquid Sprays*, Ph. D. Thesis, Princeton University.

Park, K., 1994, Development of a Non-Orthogonal-Grid Computer Code for the Optimization of Direct-Injection Diesel Engine Combustion Chamber Shapes, Ph. D. Thesis, UMIST, UK.

Reitz, R. D. and Diwakar, R., 1987, "Structure of High-Pressure Fuel Sprays," SAE870598.

Reynolds, W. C., 1980, *Modeling of Fluid Motions in Engines-an Introductory Overview, in Combustion Modeling in Reciprocating Engines*, ed. J. N. Mattavi and C. A. Amann, Plenum Press, NY.

Saito, A., Kawamura, K., Watanabe, S., Takahashi, T., and Tuzuki, N., 1993, Analysis of Impinging Spray Characteristics under High-Pressure Fuel Injection (1st Report, Measurements of Impinging Spray Characteristics), *Transaction of Japanese Society Mechanical Engineering*, Part B., Vol. 59, pp. 3290~3295.

Stanton, D. W. and Rutland, C. J., 1996, "Modeling Fuel Film Formation and Wall Interaction in Diesel Engines," SAE960628.

Wachters, L. H. J and Westerling, N. A. J., 1966, "The Heat Transfer from a Hot Wall to Impinging Water Drops in a Spherical State," *Chemical Engineering Science*, Vol. 21, pp. 1047~1056.

Watkins, A. P. and Wang, D. M., 1990, "A New Model for Diesel Spray Impaction on Walls and Comparison with Experiment," *COMODIA 90 Proceedings of International Symposium on Diagnostics and Modeling of Combustion in Internal Combustion Engines*, pp. 243~248, Kyoto, Japan.

Xiong, T. Y. and Yuen, M. C., 1991, "Evaporation of a Liquid Droplet on a Hot Plate," *International Journal of Heat and Mass Transfer*, Vol. 34, pp. 1881~1894.

Yarin, A. L. and Weiss, D. A., 1995, "Impact of Drops on Solid Surfaces: Self-Similar Capillary Waves, and Splashing as a New Type of Kinematic Discontinuity," *Journal of Fluid Mechanics*, Vol. 283, pp. 141~173.

Yoshikawa, Y., Nakada, T., Itoh, T., and Takagi, T., 1993, "Numerical Simulation System for Analyzing Fuel Film Flow in Gasoline Engine," SAE 930326.

Zahdeh A. K., Henein N., and Bryzik W., 1990, "Diesel Cold Starting: Actual Cycle Analysis Under Border-Line Conditions," SAE900441.

Zhengbai, L., Jingwei, Z., and Yueshang, L., 1990, "Experimental Investigation of Film-Space Atomization Combustion in DI Diesel Engines," SAE901578.